Molecular Structure, Acidic Properties, and Kinetic Behavior of the Cationic Complex (Methyl)(dimethyl sulfoxide)(bis-2-pyridylamine)platinum(II) Ion

Raffaello Romeo,*,‡ Nicola Nastasi,‡ Luigi Monsù Scolaro,‡ Maria Rosaria Plutino,‡ Alberto Albinati,# and Alceo Macchioni†

Dipartimento di Chimica Inorganica, Chimica Fisica e Chimica Analitica, Università di Messina and Istituto di Chimica e Tecnologia dei Prodotti Naturali (ICTPN-CNR), Sezione di Messina, Vill. S. Agata, Salita Sperone, 31. 98166 Messina, Italy, Istituto di Chimica Farmaceutica e Tossicologica, Università di Milano, Italy, and Dipartimento di Chimica, Università di Perugia, Italy

Received April 13, 1998

The complex $[PtMe(dpa)(Me_2SO)]^+(CF_3SO_3)^-$ (dpa = bis(2-pyridyl)amine) crystallizes in the monoclinic space group $P2_1/c$ with $a = 11.010(2)$ Å, $b = 18.366(2)$ Å, $c = 10.333(5)$ Å, $\beta = 111.62(2)°$, and $Z = 4$. Least-squares refinement of the structure led to an R factor of 2.41%. To avoid steric repulsions, the chelate six-membered ring assumes a boat configuration in which the two pyridyl rings are folded with a dihedral angle of 46.4(1)°. There is a strong hydrogen-bonding interaction involving the amine hydrogen (N3) and a triflate anion oxygen O3, 2.898(5) Å. The tendency by the NH group of the ligand moiety to attract anions is maintained in a solution of nonpolar solvents. Tight ion-pairs of structure similar to that in the solid state are formed with PF_6^-, BF_4^-, $CF_3SO_3^-$, and Cl^- in chloroform, as shown by the strong dependence of the chemical shifts of the NH, H(3), and H(3′) protons of the dpa ligand on the nature of the counterion. $^{19}F\{^1H\}$ HOESY experiments on $[PtMe(dpa)(Me_2SO)]^+(PF_6)^-$ in CD_2Cl_2 confirmed that the preferential position of the counterion is close to the NH proton. The absorption spectra are also strongly affected by the nature of the counterion. This allowed for a stopped-flow measure of the PF_6^- for Cl^- exchange rate at the NH site, which is a bimolecular process with $k_2 = 96.4 \pm 4\ M^{-1}\ s^{-1}$. The cation $[PtMe(dpa)(Me_2SO)]^+$ shows acidic properties in water ($pK_a = 12.1 \pm 0.2$, at 25 °C, $\mu = 0.1$ M, $NaNO_3$), and the corresponding amido species [PtMe(dpa-H)(Me_2SO)] can be isolated on basification. Ion-pairing and full deprotonation of the amine ligand have remarkably little effect on the reactivity, as shown by the comparison of the rates of isotopic exchange of dimethyl sulfoxide of these species followed by ^1H NMR in chloroform. The rates of substitution of dimethyl sulfoxide from $[PtMe(dpa)(Me_2SO)]^+$ by various charged nucleophiles were measured in methanol, where ion-pairing effects are absent, and compared with those of the parent $[PtMe(phen)(Me_2SO)]^+$ (phen = 1,10-phenanthroline) complex. Because of the reduced capacity of electron withdrawal from the metal of the ancillary ligand, the dpa complex is less reactive and possesses a minor nucleophilic discrimination ability compared with the phen complex.

Introduction

Transition-metal complexes containing chelating heterocyclic nitrogen-donor ligands have been intensively studied for many years.[1] These complexes still find widespread interest as species with promising properties in various fields, such as photochemistry, photophysics, chemiluminescence, electro-chemiluminescence, and electron-transfer chemistry[2] and for their ability to interact with molecules of biological relevance.[3] Even though a variety of platinum(II) complexes have been prepared with the familiar 2,2′-bipyridine (bpy) ligand,[4] very few are known with the bis(2-pyridyl)amine (dpa) ligand, which contains two pyridyl groups separated by a bridging NH group. Cationic complexes of formula $[Pt(AA)(dpa)]^+$ (AA is an anion of glycine or L-alanine) were shown to exhibit potential antitumor activity.[5] The introduction of a spacer group between the pyridine rings is expected to produce remarkable differences in the properties of complexes containing bpy and dpa. Unlike bpy the dpa ligand, upon coordination with the metal in a square planar configuration, forms a nonplanar six-membered ring.[6]

‡ Università di Messina and Istituto di Chimica e Tecnologia dei Prodotti Naturali.

Università di Milano.

† Università di Perugia.

(1) (a) Reedijk, J. In *Comprehensive Coordination Chemistry*, Wilkinson, G., Ed.; Pergamon: Oxford, U.K., 1987; Vol. 2, pp 73−98. (b) Constable, E. C. *Polyhedron* **1983**, *2*, 551.

(2) (a) Balzani, V.; Scandola, F. *Supramolecular Photochemistry;* Horwood, Chichester, U.K., 1991. (b) Juris, A.; Balzani, V.; Barigelletti, F.; Campagna, S.; Belser, P.; von Zelewsky, A. *Coord. Chem. Rev.* **1988**, *84*, 85. (c) Pellizzetti, E., Schiavello, M., Eds. *Photochemical Conversion and Storage of Solar Energy*; Kluwer: Dordrecht, 1991. (d) Roundhill, D. M.; Gray, H. B.; Che, C.-M. *Acc. Chem. Res.* **1989**, *22*, 55. (e) Nocera, D. G. *Acc. Chem. Res.* **1995**, *28*, 209.

(3) (a) Lippard, S. J.; Bond, P. J.; Wu, K. C.; Bauer, W. R. *Science* **1976**, *194*, 726−727. (b) Howe-Grant, M.; Wu, K. C.; Bauer, W. R.; Lippard, S. J. *Biochemistry* **1976**, *15*, 4339−4346. (c) Jennette, K. W.; Gill, J. T.; Sadownick, J. A.; Lippard, S. J. *J. Am. Chem. Soc.* **1976**, *98*, 6159−6168. (d) Arena, G.; Monsù Scolaro, L.; Pasternack, R. F.; Romeo, R. *Inorg. Chem.* **1995**, *34*, 2994. (e) Liu, H.-Q.; Peng, S.-M.; Che, C.-M. *J. Chem. Soc., Chem. Commun.* **1995**, 509.

(4) (a) Palocsay, F. A.; Rund, J. V. *Inorg. Chem.* **1969**, *8*, 524. (b) Chaudhury, N.; Puddephatt, R. J. *J. Organomet. Chem.* **1975**, *84*, 105. (c) Rendina, L. M.; Puddephatt, R. J. *Chem. Rev.* **1997**, *97*, 1735. (d) Romeo, R.; Alibrandi, G.; Arena, G.; Monsù Scolaro, L.; Plutino, M. R. *Inorg. Chim. Acta* **1995**, *235*, 281. (e)Yang, L.; Wimmer, F. L.; Wimmer, S.; Zhao, J. X.; Braterman, P. S. *J. Organomet. Chem.* **1996**, *525*, 1. (f) Collison, D.; Mabbs, F. E.; McInnes, E. J. L.; Taylor, K. J.; Welch, A. J.; Yellowlees, L. J. *J. Chem. Soc., Dalton Trans.* **1996**, 329. (g) Minniti, D. *J. Chem. Soc., Dalton Trans.* **1993**, 1343 (h) Klein, A.; Hausen, H.-D.; Kaim, W. *J. Organomet. Chem.* **1992**, *440*, 207.

10.1021/ic980423q CCC: $15.00
Published on Web 09/24/1998

In platinum(II) complexes, lack of planarity and loss of aromatization of ancillary ligands is expected to lead to a reduction of the reactivity.[7] Easy back-donation from filled d orbitals on the metal to empty antibonding orbitals of the planar ligands, such as the α-diimines 2,2′-bipyridine or phenanthroline, favors the attack of a nucleophile and increases the ability of the metal to stabilize intermediates of higher coordination number.

Searching for a correlation between the lability of substrates, the nature of the ancillary ligands, and potential catalytic properties, we studied the structure−reactivity relationship for cationic $[PtMe(N-N)(Me_2SO)]^+$ complexes, where N−N represents chelating diamines or diimines of different steric and electronic characteristics.[7] A fine-tuning of the properties of the "spectator" dinitrogen ligands led to platinum(II) substrates of very high reactivity, comparable to or even far greater than that of similar palladium(II) species. Along the series of complexes containg bpy, dpa, 2,2′-dipyridyl sulfide (dps), or pyridine (py), which have the same array of donor atoms around the metal but different orientation of the pyridine aromatic rings, the lability of dimethyl sulfoxide decreases in the order 1 (bpy), 0.33 (dpa), 0.1 (py), 0.063 (dps). Following on these results, we thought it could be worthwhile to exploit the acidic properties of the secondary amino proton of the coordinated dpa ligand[8,25a,b] to synthesize the complex $[PtMe(dpa\text{-}H)(Me_2SO)]$, where the deprotonated dpa-H ligand could have higher planarity and π-acceptor ability than dpa. Moreover we were interested in investigating the ability of dpa-H in labilizing the sulfoxide molecule.

In the course of the study, we became aware that the NH group of the dpa ligand in the organometallic cationic moiety has a strong tendency to attract anionic X^- ligands in the solid state and in nonpolar solvents with formation of tight ion-pairs. The nature of the counteranion X^- affects markedly the spectroscopic characteristics of the platinum cation $[PtMe(dpa)(Me_2SO)]^+$, and the interaction NH- -X^- is strong enough to allow the measure of the rates of anion (Cl^- for PF_6^-) exchange at the NH site using conventional spectrophotometric techniques. In view of the paucity of kinetic studies of the effect of ion-paring[9] and of amine deprotonation[10] on square planar complexes, we measured the substitutional lability of dimethyl sulfoxide for the ion-pairs $[PtMe(dpa)(Me_2SO)]^+X^-$ ($X^- = PF_6^-$, BF_4^-, $CF_3SO_3^-$) and for $[PtMe(dpa\text{-}H)(Me_2SO)]$. The results of this investigation are reported in this paper.

Experimental Section

Instrumentation. pH measurements were obtained using an Orion combined glass electrode on a Radiometer pHM62 instrument. IR spectra were recorded as Nujol mulls using a Perkin-Elmer FT-IR model 1730 spectrophotometer. One- and two-dimensional NMR spectra were measured on Bruker DRX 400, AMX R-300, and AC 200 spectrometers. Referencing was relative to Me_4Si for ^1H and for ^{13}C and H_3PO_4 (85% in D_2O) and CCl_3F for ^{31}P and ^{19}F, respectively. NMR samples were prepared dissolving about 20 mg of compound in 0.5 mL of anhydrous $CDCl_3$ or CD_2Cl_2. The temperature within the probe was checked using the methanol or ethylene glycol method.[11] The dpa ^1H and ^{13}C spectra were assigned using standard 2D homonuclear and heteronuclear correlation techniques. Two-dimensional $^{19}F\{^1H\}$ HOESY spectra were measured using a mixing time of 600 ms. UV/vis electronic spectra were recorded on a Cary 219 or a Hewlett-Packard HP8452 diode array spectrophotometer. Slow reactions were carried out in a silica cell in the thermostated cell compartment of the spectrophotometer, with a temperature accuracy of ±0.02 °C. The fastest reactions required the use of a Hi-Tech SF-3L stopped-flow apparatus, equipped with a grating monochromator and interfaced with a Pentium computer.

Materials. K_2PtCl_4 (Strem) was purified by dissolving it in water and filtering. Tetrabutylammonium hexafluorophosphate (Aldrich Chemical Co.) was crystallized from an ethyl acetate−pentane mixture and then dried over P_2O_5 under vacuum. Tetrabutylammonium chloride (Aldrich Chemical Co.) was crystallized from anhydrous acetone and ether. Bis(2-pyridyl)amine and tetramethyltin were purchased from Aldrich Chemical Co., and their purity was checked by ^1H NMR. Solvents for synthetic procedures and kinetic runs were distilled under nitrogen from appropriate drying agents (methanol from magnesium methoxide; diethyl ether from sodium benzophenone; dichloromethane from barium oxide; dimethyl sulfoxide, at a low pressure, from CaH_2, after preliminary filtration through an alumina column) and then stored in dried, N_2-filled flasks over activated 4 Å molecular sieves. Deuterated solvents for NMR measurements were used as received from Aldrich Chemical Co. All the other chemical products were reagent grade materials and were used without further purification. Microanalysis was performed by Redox Analytical Laboratories, Milan, Italy.

Preparation of Complexes. The complex *trans*-$[PtCl(Me)(Me_2SO)_2]$ (**1**) was prepared according to Eaborn et al.[12] and was purified by several crystallizations from dichloromethane/diethyl ether mixtures. The hexafluorophosphate salt $[Pt(Me)(dpa)(Me_2SO)]PF_6$ (**2**) was prepared according to a published method.[7]

$[Pt(Me)(dpa)(Me_2SO)]PF_6$ (2). Anal. Calcd for $C_{13}H_{18}F_6N_3O_1P_1Pt_1S_1$: H, 3.00; C, 25.83; N, 6.95. Found: H, 3.10; C, 25.89; N, 7.10. IR: ν(S=O) 1136 cm^{-1}. ^{13}C NMR ($CDCl_3$): δ 152.5, 150.5 ($C_2 + C_{2'}$), 150.1, 148.0 ($C_6 + C_{6'}$), 141.1, 141.7 ($C_4 + C_{4'}$), 120.1, 119.6 ($C_5 + C_{5'}$), 116.7, 115.7 ($C_3 + C_{3'}$), 45.4 ($^2J_{PtC}$ = 82 Hz, Me_2SO), −9.4 ($^1J_{PtC}$ = 700 Hz, CH_3).

$[Pt(Me)(dpa)(Me_2SO)]CF_3SO_3$ (4). A sample of **1** (0.201 g, 0.5 mmol) was reacted in methanol (3 mL) with 0.086 g (0.5 mmol) of bis(2-pyridyl)amine(dpa). The solution turned from colorless to yellow and after 10 min of stirring, was added 0.136 g (0.53 mmol) of silver triflate. Silver chloride was removed by centrifugation, and the excess solvent was evaporated under reduced pressure. The residue was dissolved in dichloromethane, the solution was filtered on a cellulose column to remove residual AgCl, and the orange product (0.236 g, 84.5% yield) separated out on adding diethyl ether and cooling at −30 °C. Anal. Calcd for $C_{14}H_{18}F_3N_3O_4Pt_1S_2$: C, 27.63; H, 2.98; N, 6.91. Found: C, 27.85; H, 2.94; N 6.72. IR: ν(S=O) 1146 cm^{-1}. ^{13}C NMR ($CDCl_3$): δ 152.7 ($^2J_{PtC}$ = 14 Hz), 150.8 ($C_2 + C_{2'}$), 150.0, 147.8 ($^2J_{PtC}$ = 23 Hz) ($C_6 + C_{6'}$), 141.4, 140.8 ($C_4 + C_{4'}$), 119.7, 119.3 ($C_5 + C_{5'}$), 116.7, 115.7 ($C_3 + C_{3'}$), 45.5 ($^2J_{PtC}$ = 84 Hz, Me_2SO), −9.4 ($^1J_{PtC}$ = 700 Hz, CH_3).

$[Pt(Me)(dpa)(Me_2SO)]BF_4$ (3). The synthesis was accomplished in a manner similar to the preparation of **4** (0.244 g, 89.4% yield). Anal. Calcd for $C_{13}H_{18}B_1F_4N_3O_1Pt_1S_1$: C, 28.58; H, 3.32; N, 7.69. Found: C, 28.53; H, 3.36; N, 7.82. IR: ν(S=O) 1131 cm^{-1}. ^{13}C NMR ($CDCl_3$): δ 152.6, 150.7 ($C_2 + C_{2'}$), 150.0, 147.8 ($C_6 + C_{6'}$), 141.6, 141.0 ($C_4 + C_{4'}$), 119.9, 119.5 ($C_5 + C_{5'}$), 116.9, 115.9 ($C_3 + C_{3'}$), 45.4 ($^2J_{PtC}$ = 84 Hz, Me_2SO), −9.5 ($^1J_{PtC}$ = 700 Hz, CH_3).

$[Pt(Me)(dpa)(Me_2SO)]Cl$ (5). This complex was prepared in situ by adding the stoichiometric amount of bis(2-pyridyl)amine to a sample

(5) Paul, A. K.; Mansuri-Torshizi, H.; Srivastava, T. S.; Chavan, S. J.; Chitnis, M. P. *J. Inorg. Biochem.* **1993**, *50*, 9.
(6) McWhinnie, W. R. *Coord. Chem. Rev.* **1970**, *5*, 293.
(7) Romeo, R.; Monsù Scolaro, L.; Nastasi, N.; Arena, G. *Inorg. Chem.* **1996**, *35*, 5087.
(8) Geldard, J. F.; Lions, F. *J. Am. Chem. Soc.* **1962**, *84*, 2262.
(9) (a) Romeo, R.; Arena, G.; Monsù Scolaro, L.; Plutino, M. R. *Inorg. Chim. Acta* **1995**, *240*, 81. (b) Alibrandi, G.; Romeo, R.; Monsù Scolaro, L.; Tobe, M. L. *Inorg. Chem.* **1992**, *31*, 3061. (c) Yagyu, T.; Aizawa, S.; Hatano, K.; Funahashi, S. *Bull. Chem. Soc. Jpn.* **1996**, *69*, 1961. (d) Wendt, O. F.; Kaiser, N.-F. K.; Elding, L. I. *J. Chem. Soc., Dalton Trans.* **1997**, 2073.
(10) (a) Romeo, R.; Minniti, D.; Alibrandi, G.; De Cola, L.; Tobe, M. L. *Inorg. Chem.* **1986**, *25*, 1944. (b) Baddley, W. H.; Basolo, F. *Inorg. Chem.* **1964**, *5*, 1087.
(11) (a) Van Geet, A. L. *Anal. Chem.* **1968**, *40*, 2227. (b) Van Geet, A. L. *Anal. Chem.* **1970**, *42*, 679.
(12) Eaborn, C.; Kundu, K.; Pidcock, A. J. *J. Chem. Soc., Dalton Trans.* **1981**, 933.

of **1** dissolved in CH_2Cl_2 or $CDCl_3$. Alternatively, this complex can be obtained by adding at least 1 equiv of Bu^n_4NCl to a solution of **2** in the same solvents.

[Pt(Me)(dpa-H)(Me$_2$SO)] (6). To 0.060 g (0.1 mmol) of **2** suspended in water (3 mL) was added 0.600 g (15 mmol) of solid NaOH. On basification, the solution turned to yellow and the precipitate that immediately separated out was collected, washed with few drops of water, and eventually dried under reduced pressure (0.042 g, 92.9% yield). IR: ν (S=O) 1123 cm^{-1}. ^{13}C NMR ($CDCl_3$): δ 156.3 ($^2J_{PtC}$ = 14 Hz), 155.7 ($C_2 + C_{2'}$), 149.0, 146.6 ($^2J_{PtC}$ = 24 Hz) ($C_6 + C_{6'}$), 136.7, 136.1 ($C_4 + C_{4'}$), 121.3 ($^3J_{PtC}$ = 18 Hz), 120.5 ($C_5 + C_{5'}$), 113.1 ($^3J_{PtC}$ = 17 Hz), 112.3 ($^3J_{PtC}$ = 46 Hz) ($C_3 + C_{3'}$), 45.2 ($^2J_{PtC}$ = 78 Hz, Me_2SO), −9.1 ($^1J_{PtC}$ = 699 Hz, CH_3).

[PtCl(Me)(dpa)] (7). A 0.200 g (0.5 mmol) sample of **1** in $CHCl_3$ (5 mL) was reacted with 0.086 g (0.5 mmol) of bis(2-pyridyl)amine. The solution was stirred at 50 °C for 1 day. The yellow precipitate that separated out was collected and washed with diethyl ether (0.184 g, 88.6% yield). ^{1}H NMR (acetone-d_6): δ 9.63 (s, 1H), 9.06 (dd, $^3J_{PtH}$ = 20 Hz, 1H), 8.57 (dd, $^3J_{PtH}$ = 59.4 Hz, 1H), 7.95 (t, 1H), 7.86 (t, 1H), 7.25 (dt, 2H), 7.06 (t, 1H), 7.00 (t, 1H), 0.82 (s, $^2J_{PtH}$ = 78.0 Hz, 3H). Anal. Calcd for $C_{11}H_{12}Cl_1N_3Pt_1$: C, 31.70; H, 2.90; N, 10.08. Found: C, 31.65; H, 2.87; N, 10.15.

pK_a Determination. Complex **2** was dissolved to a concentration of 20 μM in 100 mL of distilled water (μ = 0.1 ($NaNO_3$), 25 °C). The pH was raised in ~0.1 pH units increments by adding small amounts of 4.0 M NaOH with magnetic stirring. Two milliliters of solution were withdrawn after each addition, the UV−visible absorption spectrum was recorded, and the aliquot was returned to the original container. At any suitable wavelength in the range 350−450 nm, addition of NaOH leads to a considerable increase in absorbance, the plot of absorbance vs pH having the typical sigmoid form of a titration curve (Figure S1 in the Supporting Information). A value of pK_a = 12.1 ± 0.2 was evaluated by a best fitting analysis of the absorbance data at the λ_{max}, using the SCIENTIST program.[13]

X-ray Data Collection and Structure Refinement. Crystals of [PtMe(dpa)(Me$_2$SO)]CF_3SO_3 (**4**), suitable for X-ray diffraction study, were grown by slow evaporation of concentrated dichloromethane solutions. A colorless crystal of **4** was mounted on a CAD4 diffractometer that was used for the unit cell and space group determination and for data collection. Unit cell dimensions were obtained by least-squares fit of the 2θ values of 25 high-order reflections (9.47° ≤ θ ≤ 18.03°). Selected crystallographic and other relevant data are listed in Table 1 and in Table S1 in the Supporting Information. Data were measured with variable scan speed to ensure constant statistical precision on the collected intensities. Three standard reflections were used to check the stability of the crystal and of the experimental conditions and measured every hour; no significant variation was detected. Data were corrected for Lorentz and polarization factors using the data reduction programs of the MOLEN crystallographic package.[14] An empirical absorption correction was also applied (azimuthal (Ψ) scans of three reflections having χ > 86°).[15] The standard deviations on intensities were calculated in terms of statistics alone, while those on F_o were calculated as shown in Table 1.

The structure was solved by a combination of direct and Fourier methods and refined by full-matrix least-squares. During the final refinement anisotropic displacement parameters were used for all atoms. The contribution of the hydrogen atoms, in idealized positions (C−H = 0.95 Å, $B = 1.5B_{(bonded\ atom)}$ Å^2), was taken into account but not refined. The function minimized was $[\Sigma w(|F_o| - 1/k|F_c|)^2]$. No extinction correction was deemed necessary. The scattering factors used, corrected for the real and imaginary parts of the anomalous dispersion, were taken from the literature.[16] Upon convergence the final Fourier difference map showed no significant peaks. All calculations were carried out using the Enraf-Nonius MOLEN crystallographic programs.[14]

Table 1. Experimental Data for the X-ray Diffraction Study of Compound [PtMe(dpa)(Me$_2$SO)]CF_3SO_4 (**4**)

chem formula	$C_{14}H_{18}F_3O_4N_3PtS_2$
mol wt	608.53
data coll T, °C	23
cryst syst	monoclinic
space group	$P2_1/c$ (No. 14)
a, Å	11.010(2)
b, Å	18.366(2)
c, Å	10.333(3)
β, deg	111.62(2)
V, Å^3	1941(1)
Z	4
ρ(calcd), g cm^{-3}	2.081
μ, cm^{-1}	75.566
radiation	Mo Kα (graphite monochromated)
θ range, deg	2.5 < θ < 26.5
no. obs reflct (n_o) ($F^2_o > 3.0\sigma(F^2)$)	3177
transmission coeff	0.9964−0.6287
no. of params refined (n_v)	244
R[a]	0.024
R_w[b]	0.033
GOF[c]	1.622

[a] $R = \sum(|F_o - (1/k)F_c|)/\sum|F_o|$. [b] $R_w = [\sum_w(F_o - (1/k)F_c)^2/\sum_w|F_o|^2]^{1/2}$. $w = [\sigma^2(F_o)]^{-1}$. $\sigma(F_o) = [\sigma^2(F_o^2) + f^4(F_o^2)]^{1/2}\ 2F_o$. [c] GOF = $[\sum w(F_o - (1/k)F_c)^2/(n_o - n_v)]^{1/2}$.

Table 2. Selected Bond Distances (Å), Bond Angles (deg), and Torsion Angles (deg) for [PtMe(dpa)(Me$_2$SO)](CF_3SO_3) (**4**)

Pt−N(1)	2.063(4)	C(2)−N(3)	1.377(6)
Pt−N(2)	2.133(4)	C(2′)−N(3)	1.402(6)
Pt−S(1)	2.197(1)	S(1)−O(1)	1.480(4)
Pt−C(7)	2.049(5)	S(1)−C(8)	1.765(5)
N(1)−C(2)	1.340(5)	S(1)−C(9)	1.775(6)
N(2)−C(2′)	1.334(5)	N(3)···O(4)	2.898(5)

N(1)−Pt−N(2)	83.6(1)	Pt−N(2)−C(2′)	117.8(3)
N(1)−Pt−S(1)	175.88(9)	N(3)−C(2′)−N(2)	118.0(4)
N(1)−Pt−C(7)	90.2(2)	Pt−S(1)−O(1)	115.0(2)
N(2)−Pt−S(1)	96.4(1)	Pt−S(1)−C(8)	113.5(2)
N(2)−Pt−C(7)	173.7(2)	Pt−S(1)−C(9)	111.1(2)
S(1)−Pt−C(7)	89.8(1)	O(1)−S(1)−C(8)	108.2(2)
Pt−N(1)−C(2)	118.7(3)	O(1)−S(1)−C(9)	108.0(3)
N(1)−C(2)−N(3)	119.4(4)	C(8)−S(1)−C(9)	99.9(2)
C(2)−N(3)−C(2′)	122.4(3)		

S(1)−Pt−N(1)−C(6)	−130(1)
S(1)−Pt−N(2)−C(6′)	42.7(4)
C(7)−Pt−N(1)−C(6)	−39.2(4)
C(7)−Pt−N(2)−C(6′)	−145(1)
Pt−N(1)−C(2)−N(3)	10.9 (5)
Pt−N(2)−C(2′)−N(3)	−13.8(5)
C(9)−S(1)−Pt−N(1)	35(2)

Kinetics: (i) Counterion Exchange. The PF_6^- for Cl^- exchange rates at the NH site of the dpa ligand were followed in CH_2Cl_2 by means of stopped-flow techniques. The temperature was controlled to within ±0.02 °C through a temperature sensor attached to the base of the cell housing. Initial concentration of starting complex **2** was 0.05 mM. The concentration of Bu^n_4NCl was at least a 10-fold excess over the complex to ensure pseudo-first-order kinetics in any run. The time-resolved spectra, taken at the wavelength where the spectral change was largest, were stored on the computer and fitted to the equation $A_t = A_\infty + (A_0 - A_\infty)\exp(-k_{obsd}t)$ with A_0, A_∞, and k_{obsd} as the parameters to be optimized (A_0 = absorbance after mixing of reagents, A_∞ = absorbance at completion of reaction). The pseudo-first-order rate constants k_{obsd} are reported in Table 4 as average values from five to seven independent runs.

(**ii**) **Dimethyl Sulfoxide Exchange.** The kinetics of isotopic exchange were performed by adding with a microsyringe a known volume of dimethyl sulfoxide-d_6 on a prethermostated solution of

(13) *SCIENTIST*; Micro Math Scientific Software: Salt Lake City, UT.
(14) *MOLEN* Enraf-Nonius Structure Determination Package; Enraf-Nonius: Delft, The Netherlands, 1990.
(15) North, A. C. T.; Phillips, D. C.; Mathews, F. S. *Acta Crystallogr., Sect. A* **1968**, *24*, 351.
(16) *International Tables for X-ray Crystallography*; Kynoch: Birmingham, England, 1974; Vol. IV.

Table 3. ^{1}H NMR Data for [PtMe(dpa)(Me$_2$SO)](X) and [PtMe(dpa-H)(Me$_2$SO)] Complexes[a]

no.	X$^-$	δ(CH$_3$Pt)	δ(Me$_2$SO)	δ(H$^{3,3'}$)	δ(H$^{4,4'}$)	δ(H$^{5,5'}$)	δ(H$^{6,6'}$)	δ(N−H)
2	PF_6^-	0.58 (72.6)	3.38 (34.1)	7.73	7.89	7.14	8.10 (46.2); 8.56 (17.6)	9.03
3	BF_4^-	0.56 (72.6)	3.38 (34.6)	7.78	7.86	7.10	8.08 (46.2); 8.54 (∼22)	9.71
4	$CF_3SO_3^-$	0.56 (73.0)	3.37 (33.2)	7.84	7.84	7.10	8.07 (46.4); 8.54 (23.0)	10.5
5	Cl^-	0.54 (72.6)	3.35 (34.0)	8.32	7.80	7.04	8.03 (45.4); 8.51 (22.0)	12.69
6		0.40 (71.4)	3.24 (29.8)	6.87; 7.00	7.29; 7.40	6.35; 6.53	7.67 (49); 8.29 (∼11)	

[a] In chloroform-*d*. Chemical shifts are reported in parts per million units from Me$_4$Si at 298 K. $^2J_{PtH}$ for PtCH$_3$ and $^3J_{PtH}$ for Pt(CH$_3$)$_2$SO and the aromatic protons are given in Hz in parentheses.

Table 4. Pseudo-First-Order Rate Constants and Second-Order Rate Constant for Counterion Exchange (Hexafluorophosphate for Chloride) at the NH Site of the dpa Ligand in the [PtMe(dpa)(Me$_2$SO)]$^+$ Cation[a]

[Cl$^-$]/mM	k_{obsd}[b]	k_2[c]
0.5	0.073	96.4 ± 4
2.5	0.218	
3.75	0.340	
5.0	0.423	
7.5	0.785	
12.5	1.29	
25.0	2.37	

[a] In dichloromethane at 301 K. [b] s^{-1}. [c] M^{-1} s^{-1}. [Complex, **2**] = 0.05 mM.

weighted [PtMe(dpa)(Me$_2$SO)]X (X = PF_6^- (**2**), BF_4^- (**3**), $CF_3SO_3^-$ (**4**)) complex in acetone-d_6 or chloroform-*d*. At least a 5-fold excess of Me$_2$SO-d_6 over the complex was ensured in any run. All concentrations are expressed in moles per kilogram of solvent (m = mol kg^{-1}). The isotopic exchange was followed by monitoring the increase in intensity of the proton NMR signal of free Me$_2$SO and the matching decrease of the signal of the sulfoxide coordinated to the metal. The spectra were recorded at appropriate time intervals. The same procedure was followed for the amido complex [PtMe(dpa-H)(Me$_2$SO)] (**6**) in chloroform-*d*. The mole fraction $F = [Me_2SO]_f/([Me_2SO]_f + [Me_2SO]_b)$ of the free nondeuterated dimethyl sulfoxide was obtained by integration of the signals, and the first-order rate constants k_{exch} (s^{-1}) for the exchange of the label were obtained from a nonlinear least-squares fit of the experimental data to $F = c_1 + c_2 \exp(-k_{exch}t)$, with c_1, c_2, and k_{exch} as the parameters to be optimized. A similar analysis can be performed by using the mole fraction of the nondeuterated bound dimethyl sulfoxide. From the McKay equation, $R_{exch} = k_{exch}ab\ (a + b)^{-1}$ (where R_{exch} is the rate of the exchange process; a the concentration of complex; and b the concentration of added sulfoxide), the pseudo-first-order rate constants, $k_{obsd} = R_{exch}/a$, were calculated and collected in Table S6 in the Supporting Information.

(iii) Dimethyl Sulfoxide Substitution. The rates of Me$_2$SO for Cl^-, Br^-, I^-, and SCN^- substitution in methanol were followed spectrophotometrically by repetitive scanning of the spectrum at suitable times in the range 450−260 nm. The reactions were started by mixing equal amounts of prethermostated solutions of both reagents in a silica cell, in the thermostated cell compartment of the spectrophotometer, with a temperature accuracy of ±0.02 °C. The use of at least a 10-fold excess of nucleophile over complex ensured pseudo-first-order kinetics in all runs. The time-resolved spectra were processed with a nonlinear least-squares fitting to the first-order rate equation, as described before for counterion exchange. The pseudo-first-order rate constants k_{obsd} as a function of nucleophile concentration are reported in Table S7 in the Supporting Information.

Results and Discussion

The complexes [PtMe(dpa)(Me$_2$SO)]$^+$X$^-$ (X$^-$ = PF_6^- (**2**), BF_4^- (**3**), $CF_3SO_3^-$ (**4**), and Cl^- (**5**)) were synthesized from the precursor *trans*-[PtMeCl(Me$_2$SO)$_2$] (**1**) and fully characterized by elemental analyses and IR, ^{1}H, and ^{13}C spectroscopy. Addition of excess sodium hydroxide to an aqueous solution of **2** leads to an immediate change in the spectrum. The process is reversible on acidification with $HClO_4$. A spectrophotometric pH titration gave pK_a = 12.1 ± 0.2 at 25 °C. The fully deprotonated complex [Pt(dpa-H)(Me$_2$SO)(CH$_3$)] (**6**) was prepared by basification of concentrated solutions of **2** in water.

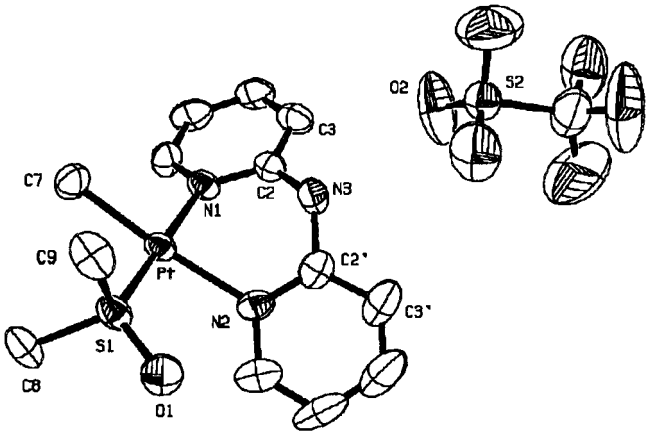

Figure 1. ORTEP drawing of [PtMe(dpa)(Me$_2$SO)]CF_3SO_3, showing the labeling of the non-H atoms. Thermal ellipsoids are drawn at the 40% probability level.

Crystal Structure. An ORTEP view of compound **4** is given in Figure 1, while selected bond distances and angles are listed in Table 2. To the best of our knowledge, the cation is the first of this type to be structurally characterized. The crystal structure is constituted by discrete cationic moieties and triflate anions held together by hydrogen bonds (vide infra) and van der Waals forces. The coordination around the platinum in the cation is approximately square planar with a small bisphenoidal distortion. The immediate coordination sphere contains the two nitrogens of the dpa ligand, the sulfur of the dimethyl sulfoxide, and the carbon of the methyl group. The Pt−C bond length (2.049(5) Å) is in the range of values reported for a number of platinum complexes.[17] The Pt−S distance (2.197(1) Å) agrees well with the value expected on the basis of the trans influence order O < N ≈ Cl < S < C established for the Pt−Me$_2$SO bond length.[18] Moreover, it is significantly shorter than those observed for *trans*-[PtMeCl(Me$_2$SO)$_2$] (2.261−2.257)[18] and for *cis*-[PtPh$_2$(Me$_2$SO)$_2$] (2.315−2.324 Å)[19] and comparable to those observed for Pt−Me$_2$SO distances trans to chloride (2.185−2.233 Å) and trans to nitrogen (2.209−2.224 Å).[20] The Pt−N(2) bond distance (2.133(4) Å) for the nitrogen in trans position to the strong σ-donor Pt−C bond is comparable to that of *cis*-[PtPh$_2$(CO)(py)] (2.140(4) Å)[21] and, as expected on the basis of the trans influences of the methyl and Me$_2$SO groups, is significantly longer than that of Pt−N(1) (2.063(4) Å).

(17) Cambridge Structural Data Base (1992−1997). Cambridge Crystallographic Data Centre, 12 Union Road, Cambridge, England.
(18) Romeo, R.; Monsù Scolaro, L.; Nastasi, N.; Mann, E. M.; Bruno, G.; Nicolò, F. *Inorg. Chem.* **1996**, *35*, 7691.
(19) Alibrandi, G.; Bruno, G.; Lanza, S.; Minniti, D.; Romeo, R.; Tobe, M. L. *Inorg. Chem.* **1987**, *26*, 185.
(20) Caligaris, M.; Carugo, O. *Coord. Chem. Rev.*, **1996**, *153*, 1−23.
(21) Romeo, R.; Arena, G.; Monsù Scolaro, L.; Plutino, M. R.; Bruno, G.; Nicolò, F. *Inorg. Chem.* **1994**, *33*, 4029.

All the bond distances in the coordination plane of **4** have values comparable to those found in the parent complex [Pt(phen)(Me_2SO)(CH_3)] (Pt−C, 2.049(7) Å; Pt−S, 2.203(1) Å; Pt−N(1), 2.075(4) Å; and Pt−N(2), 2.135(4) Å), where the 1,10-phenanthroline ligand is planar and coordinates to the Pt atom with a bite angle of 79.3(2)°.[22] The chelate ring in **4**, defined by the atoms Pt, N(1), C(2), N(3), C(2′), and N(2), is in a boat configuration, and its bite angle N(1)−Pt−N(2) is 83.6(1)°. The plane defined by N(1), C(2), C(2′), and N(2) and the coordination plane (defined by S(1), C(7), Pt, N(1), and N(2)) make an angle of 42.1(2)°. The distortion of the dpa ligand is shown by the dihedral angle of 46.4(1)° between the two pyridyl rings. The pyridyl rings themselves are not strictly planar, with deviations from the least-squares planes defined by the six atoms of *c*/*a* ± 0.3 Å. Worthy of note is the presence of a strong hydrogen-bonding interaction between the amine hydrogen N(3) and the triflate anion oxygen O(3), 2.898(5) Å.

NMR Measurements. The ^{1}H NMR data for complexes **2**−**6** are collected in Table 3. The spectrum of **2** shows signals due to Me_2SO at δ 3.38 ($^3J_{PtH}$ = 34.1 Hz), to the methyl group at δ 0.58 ($^2J_{PtH}$ = 72.6 Hz) and to the NH group at δ 9.03. The aromatic protons H_6 and $H_{6'}$ can be distinguished on the basis of the magnitude of the coupling constants with ^{195}Pt. The H_6 proton (trans to Me_2SO) shows a coupling constant much larger ($^3J_{PtH}$ = 46.2 Hz) than that observed for the $H_{6'}$ proton (trans to CH_3; $^3J_{PtH}$ = 17.6 Hz). This criterion of peak assignment, based on the different trans influence of methyl and Me_2SO, has been successfully applied to establish the geometrical configuration of [PtMeCl(Me_2SO)(am)] (am = amines or pyridines) isomers.[18] Signals due to $H_{3,3'}$, $H_{4,4'}$, and $H_{5,5'}$ were assigned on the basis of proton−proton coupling constants, proton−platinum coupling constants, and H−H COSY.

The six-membered ring, formed by the coordination of the two nitrogens of the ligand (Figure 1), assumes a conformation in which the N(3) atom lies well outside the square planar coordination plane. Therefore the dimethyl sulfoxide ligand should become prochiral and the two methyl groups should be diastereotopic. Thus, the single signal observed in the Me_2SO NMR region can be explained by rapid flipping of the dpa ligand, which renders the two methyl groups magnetically equivalent. A similar explanation applies for the single Me_2SO ^{1}H NMR signal found for compound **6**, which can hardly be taken as an indication of complete planarity of the coordinated bis(2-pyridyl)amine following its full deprotonation. A large distortion of the dpa ligand is required to minimize the repulsions between the hydrogen atoms H_6 and $H_{6'}$ and the groups on the coordination plane; in fact, in the palladium(II) complex [Pd(dpa-H)$_2$], the chelate rings are boat-shaped in a similar way to that described for **4**.[23]

The values of the chemical shifts for the $H_{4,4'}$ and $H_{5,5'}$ protons of the dpa ligand (Table 3) do not show any dependence on the nature of the counteranion and remain constant along the series of compounds **2**−**5** at δ 7.85 ± 0.04 and 7.09 ± 0.04, respectively. By contrast, the NH and the $H_{3,3'}$ signals undergo a remarkable downfield shift on changing the counterion in the order PF_6^- < BF_4^- < $CF_3SO_3^-$ < Cl^-, indicative of a strong interaction of the anion with the amine H atom of the dpa ligand. As an example, upon addition of a stoichiometric amount of Bu^n_4NCl to a solution of the hexafluorophosphate salt **2**, the NH signal undergoes a downfield shift from δ 9.03 to δ 12.69 and the $H_{3,3'}$ signals move from δ 7.73 to δ 8.32. These latter values do not change on adding further amounts of chloride salt. This is a straightforward indication that a cation−anion ratio of 1:1 is sufficient to form a tight ion pair, i.e., {[PtMe(dpa)(Me_2SO)]$^+$, Cl^-}.

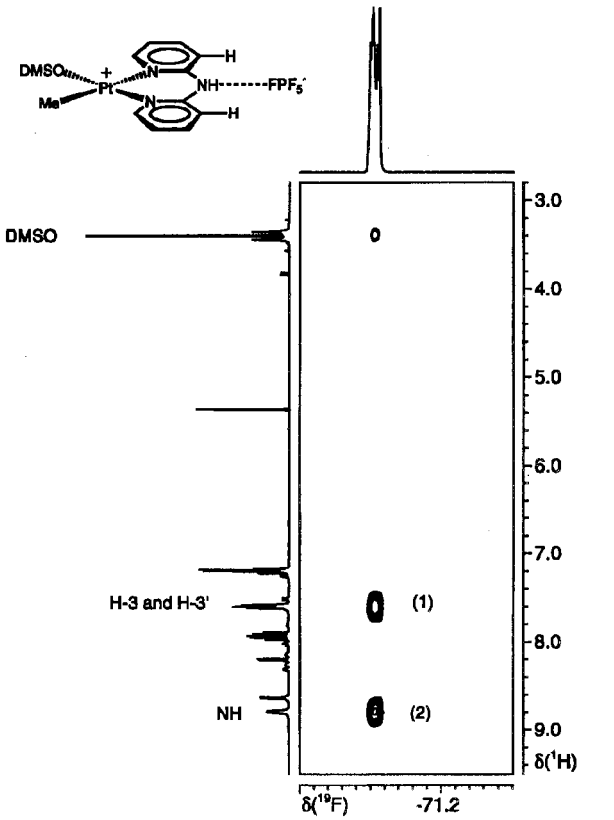

Figure 2. Section of the ^{19}F{^{1}H} HOESY spectrum of the complex [PtMe(dpa)(Me_2SO)]PF_6 recorded at 376 MHz in CD_2Cl_2. The ^{19}F projection shows only one of the two resonances due to the coupling with ^{31}P that is structured owing to the N−H···F−PF_5^- interaction. The preferential interionic contacts between PF_6^- and the N−H (2) and H-3 and H-3′ (1) protons are clearly shown.

The interaction between the counterion and the organometallic moiety in solution has been directly demonstrated by the detection of interionic contacts[24] in the ^{19}F{^{1}H} HOESY spectrum of compound [PtMe(dpa)(Me_2SO)]$^+PF_6^-$ in CD_2Cl_2. This spectrum shows strong interionic contacts between the fluorine atoms of the counterion and the N−H, H(3), and H(3′) protons of the bis(2-pyridyl)amine ligand and a weak contact with the dimethyl sulfoxide protons (Figure 2). This means that the preferential position of the counterion is close to the N−H proton and the averaged interionic solution structure is similar to that in the solid state, even for one of the less coordinating counterion, i.e., PF_6^-. Furthermore, the ^{19}F NMR spectrum appears as an apparently structured doublet (see the upper projection of the ^{19}F{^{1}H} HOESY spectrum reported in Figure 2), but the fine separation of the resonances depends on the magnetic field where the measurements have been performed. It can be deduced that the interaction of PF_6^- with the "acid" N−H proton makes the atoms of fluorine inequivalent, affording a 1:4:1 signal. This is confirmed by the ^{19}F spectrum in CD_2Cl_2 (not completely anhydrous), where the fine structure is no longer present. In this case H_2O competes with PF_6^-, and it does not allow the formation of a tight ion-pair N−H···F−PF_5^-.

(22) Bruno, G.; Nicolò, F.; Scopelliti, R.; Arena, G. *Acta Crystallogr., Sect. C* **1996**, *52*, 827.
(23) Freeman, H. C.; Snow, M. R. *Acta Crystallogr.* **1965**, *18*, 843.
(24) (a) Bellachioma, G.; Cardaci, G.; Macchioni, A.; Reichenbach, G.; Terenzi, S. *Organometallics* **1996**, *15*, 4349. (b) Macchioni, A.; Bellachioma, G.; Cardaci, G.; Gramlich, V.; Rüegger, H.; Terenzi, S.; Venanzi, L. M. *Organometallics* **1997**, *16*, 2139.

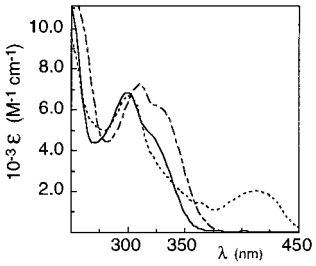

Figure 3. Absorption spectra of the compounds [PtMe(dpa)(Me$_2$SO)]-PF$_6$ (—), [PtMe(dpa)(Me$_2$SO)]Cl (- - -), and [PtMe(dpa-H)(Me$_2$SO)] (• ••) in dichloromethane solution.

Absorption Spectra. Room-temperature absorption spectra of **2**, **5**, and **6** in dichloromethane solution are presented in Figure 3. A complete set of absorption maxima together with the extimated extinction coefficients for compounds **2**−**6** are given in Table S8 in the Supporting Information. The spectra of the salts **2**−**5** show intense bands in the ultraviolet, similar to those displayed by the free ligand, which can be assigned to $\pi \rightarrow \pi^*$ spin-allowed ligand transitions. In the lower energy region (above 330 nm) these dpa complexes exhibit a long structureless tail. Similar absorptions have been observed for a number of rhodium(III) and iridium(II) dpa complexes.[25] The absorption spectrum of the yellow, fully deprotonated, complex **6** shows a band at a much lower energy (414 nm) than that observed for the protonated complexes **2**−**5**, which in turn can be assigned to a singlet charge-transfer low-energy d $\rightarrow \pi^*$ transition. This band could well be assigned to a low-energy $\pi \rightarrow \pi^*$ transition favored by aromatization of the deprotonated ligand and by extensive conjugation between the two halves of the chelate ring.

The most interesting feature in the absorption spectra of **2**−**5** is the sensitivity of the positions of the maxima to the nature of the anion. As an example, the difference between the two peaks for **2** and **5** is 1075 cm^{-1}. The phenomenon at the origin of the perturbartion of the bands and of the bathochromic shifts is the same as for the shifts of the NH and H(3,3′) proton resonances, namely, the strong hydrogen bonding N(3)H- -X$^-$ interaction, which may affect significantly the energy of the transitions.

Kinetics. (i) Rates of Anion Exchange at the N(3)H Site. The sharp change of the absorption characteristics of **2** and **5**, displayed in Figure 3, allowed for a stopped-flow spectrophotometric determination of the PF$_6^-$ for Cl$^-$ exchange rate at the N(3)H site of the dpa ligand in the cation **2** in dichloromethane solution. The rate data in Table 4 show a first-order dependence on the chloride concentration and obey the rate law $k_{obsd} = k_2[Cl^-]$. The value of k_2 at 301 K, determined from the slope of the plot of k_{obsd} vs [Cl$^-$], is 96.4 ± 4 M^{-1} s^{-1}. The most likely mechanism that can be envisaged is reminiscent of a concerted nucleophilic substitution and involves a direct bimolecular attack by the chloride on the acidic proton to remove the less tightly bound hexafluorophosphate ion. The described process can hardly be associated with the anion exchange between ion pairs held together solely by electrostatic interactions (as for Bu$^n_4$N$^+$PF$_6^-$ and Bu$^n_4$N$^+$Cl$^-$ salts, in solvents of low dielectric constant), which is a diffusion-controlled process. The process we are dealing with owes its peculiar slowness to the strength of the NH···F−PF$_5^-$ hydrogen bond which is broken as the formation of the more stable NH···Cl$^-$ hydrogen bond takes over. The attack at the N(3)H site is selective and relatively fast in comparison to the attack at the platinum(II) center. In fact a solution of [PtMe(dpa)(Me$_2$SO)]$^+$Cl$^-$ in dichloromethane is stable for hours, and only the addition of massive amounts of Bu$^n_4$NCl salt leads to a slow dimethyl sulfoxide substitution to yield [PtMeCl(dpa)].

Table 5. Second-Order Rate Constants, k_2, for Me$_2$SO Exchange on [PtMe(dpa)(Me$_2$SO)]$^+$X$^-$ and [PtMe(dpa-H)(Me$_2$SO)] Complexes in Acetone-d_6 and Chloroform-d[a]

no.	X$^-$	10^3k_2[b]
2[c,d]	PF$_6^-$	53.6 ± 0.2
4[c]	CF$_3$SO$_3^-$	48.3 ± 3
2[e]	PF$_6^-$	7.01 ± 0.5
3[e]	BF$_4^-$	6.03 ± 0.3
4[e]	CF$_3$SO$_3^-$	3.86 ± 0.3
6[e]		3.34 ± 0.1

[a] At 298 K. [b] M^{-1} s^{-1}. [c] In acetone-d_6. [d] From ref 7 [e] In chloroform *d*.

(ii) Rates of Dimethyl Sulfoxide Exchange. The systematic kinetics of dimethyl sulfoxide exchange on complexes **2**−**4** and **6** were studied in acetone and chloroform, at different Me$_2$SO concentrations, and were followed by isotopic exchange. During the exchange there was no indication of ring opening or of other concurrent processes. The dependence of the pseudo-first-order rate constants, listed in Table S6, is described by a family of straight lines (Figure S2 in the Supporting Information) and obeys eq 1:

$$k_{obs} = k_1 + k_2[Me_2SO] \qquad (1)$$

The contribution of the reagent-independent term k_1 is negligible for the cationic compounds **2**−**4** in both solvents, and it is small but detectable for the deprotonated complex **6** in chloroform. Linear regression analysis of these plots gave the values of k_2, the second-order rate constant for the bimolecular attack of Me$_2$SO on the substrate. The values of k_2 are listed in Table 5. In keeping with previous findings[7] and with the usual pattern of behavior of square planar platinum(II) complexes, the exchange takes place with an associative mode of activation. In acetone, where there is no ion-pairing effect, the values of k_2 for **2** and **4** are almost identical, being (53 ± 2) × 10^{-3} M^{-1} s^{-1} [7] and (48 ± 5) × 10^{-3} M^{-1} s^{-1}, respectively. In chloroform as solvent the lability of the sulfur-bonded Me$_2$SO in the [PtMe(dpa)(Me$_2$SO)]$^+$ cation is 6−7 times less than in acetone, and it is only slightly affected by the nature of the counteranion, decreasing in the order PF$_6^-$ > BF$_4^-$ > CF$_3$SO$_3^-$. The difference of reactivity between the first and the last members of the series is not very large (cf k_2 = (7 ± 0.5) × 10^{-3} M^{-1} s^{-1} for **2** with k_2 = (3.9 ± 0.2) × 10^{-3} M^{-1} s^{-1}for **4**), but the trend is sufficiently clear. The hierarchy of the effect of ion-pairing on the reactivity of [PtMe(dpa)(Me$_2$SO)]$^+$ reflects that found for its spectroscopic properties, and it is presumably the same as the sequence of strength of the N(3)H···X$^-$ hydrogen bonding. Hovewer, the overall effect on the reactivity is fairly modest.

A significant feature of the reactivity data is that the lability of the fully deprotonated complex **6** (k_2 = (3.3 ± 0.2) × 10^{-3} M^{-1} s^{-1}) is of the same order of magnitude of that of the ion pairs **2**−**4** in chloroform and not very much different from that of the cation [PtMe(dpa)(Me$_2$SO)]$^+$ in acetone. The most

(25) (a) Huang, W. L.; Segers, D. P.; DeArmond, M. K. *J. Phys. Chem.* **1981**, *85*, 2080. (b) Morris, D. E.; Ohsawa, Y.; Segers, D. P.; DeArmond, M. K.; Hanck, K. W. *Inorg. Chem.* **1984**, *23*, 3010. (c) McDevitt, M. R.; Ru, Y.; Addison, A. W. *Transition Met. Chem.* **1993**, *18*, 197. (d) Anderson, P. A.; Deacon, G. B.; Haarmann, K. H.; Keene, F. R.; Meyer, T. J.; Reitsma, D. A.; Skelton, B. W.; Strouse, G. F.; Thomas, N. C.; Treadway, J. A.; White, A. H. *Inorg. Chem.* **1995**, *34*, 6145.

Table 6. Second-Order Rate Constants for Dimethyl Sulfoxide Substitution from the Cation $[PtMe(dpa)(Me_2SO)]^+$ by Some Nucleophiles in MeOH at 313 K[a]

reagent	10^2k_2[b]
Cl^-	0.178 ± 0.014
Br^-	1.06 ± 0.01
I^-	47.9 ± 1
SCN^-	195 ± 2

[a] $\mu = 0.1$ M ($NaNO_3$). [b] M^{-1} s^{-1}.

significant feature that emerges is that the removal of a proton at the N(3) atom of the ligand has remarkably little effect on the reactivity of the substrate. The labilizing effect of the amido group that dominates the dissociatively activated base-catalyzed reactions of octahedral complexes,[26] especially those of Co(III), where the substitutional lability is enhanced by factors ranging from 10^5 to 10^{13}, is absent. These findings are in keeping with the results of the other few studies of the effect of amine deprotonation on the associatively activated substitution reactions of four-coordinate planar complexes of d^8 reaction centers.[10] Some of these studies were complicated by the problem of correcting the rates for primary salt effects or by contemporary ring-opening processes, but the reactivity differences derived between the amino and the amido species are reliable. As an example, $[Pt(dien)(Me_2SO)]^{2+}$ (dien = 1,5-diamino-3-azapentane) behaves as a weak acid ($pK_a = 11.94$ at 298 K), and deprotonation at the 3-nitrogen leads to a relatively small decrease in reactivity (a factor of ~2) in the reactions with various nucleophiles.[10a] Likewise, the reactivity in the amido complex was halved with respect to that of $[Au(dien)Cl]^{2+}$.[10b] As far as the solvolytic pathway for substitution is concerned, the trend seems to be opposite. $[Pt(en)(Me_2SO)_2]^{2+}$ (en = 1,2-diaminoethane) undergoes deprotonation in basic solution, but the solvolytic lability of the amido conjugate base is some 10 times greater than that of the amine species.[10a] If [PtMe(dpa-H)(Me_2SO)] bears the same pattern of behavior, its small reagent-independent term ($k_1 = (1.07 \pm 0.2) \times 10^{-4}$ s^{-1}) could be explained as a result of solvolytic attack by the adventious presence of water in the chloroform used as the solvent.

(iii) Rates of Dimethyl Sulfoxide Substitution. Preliminary experiments indicated that the rates of Me_2SO substitution from the cation $[PtMe(dpa)(Me_2SO)]^+$ with a series of negatively charged nucleophiles in methanol were independent of the nature of the counterion. The systematic kinetics were carried out using **2** as the substrate in a reagent concentration range 5−100 mM, at constant ionic strength ($\mu = 0.1$ M, $NaNO_3$). The pseudo-first-order rate constants, k_{obsd}, listed in Table S7 in the Supporting Information, when plotted against the concentration of the entering nucleophile, give straight lines with a common intercept, indicating that the usual two-term rate eq 1 is obeyed. The value of k_1 is almost negligible, and the values of the second-order rate constants k_2, obtained from linear regression analysis of the rate law, are collected in Table 6 (not corrected for the ionic strength effect). The reactivity of **2** at 313 K is still far less (~1 order of magnitude) than that of the cation $[PtMe(phen)(Me_2SO)]^+$ at 298 K; the reactivity sequence $Cl^- < Br^- < SCN^- < I^-$ differs only as far as the relative positions of I^- and SCN^- are concerned.

The cation with 1,10-phenanthroline is characterized by extensive planarity and π-acceptor properties of the ancillary ligands (both phen and Me_2SO). This complex has been shown to possess the highest capacity of nucleophilic discrimination among platinum(II) substrates bearing a +1 charge.[9a] Withdrawal of electron density by the ligands enhances the electrophilicity of the metal and favors a high degree of bond formation in the five-coordinate transition state. On plotting log k_2 for a particular nucleophile reacting with **2** against log k_2 for the same nucleophile reacting with $[PtMe(phen)(Me_2SO)]^+$, assumed as a standard, one obtains a straight line with slope = 0.856 ± 0.13 (Figure S3 in the Supporting Information). It follows that the cation $[PtMe(dpa)(Me_2SO)]^+$ not only is less reactive than the parent $[PtMe(phen)(Me_2SO)]^+$ but exhibits a minor capacity of nucleophilic discrimination. Both the reduction of reactivity and the loss of nucleophilic discrimination ability can be attributed to the presence of a "spacer group" between the pyridine rings which prevents the bidentate dpa ligand from behaving as an α-diimine. As a consequence, the ability of the metal to transfer electron density to the dinitrogen ancillary ligand decreases together with its ability to counteract the effects of the electron pair brought in by the entering nucleophile in a bimolecular substitution reaction.

Conclusions

The crystal structure of the cation $[PtMe(dpa)(Me_2SO)]^+$ shows two important features: (i) a large distortion of the dinitrogen ligand to avoid steric congestion with the other groups in the coordination plane and (ii) a strong hydrogen-bonding interaction with the counterion $CF_3SO_3^-$, through the secondary amino group which separates the two pyridyl rings of the dpa ligand. This strong tendency to attract anionic X^- species is maintaned in a solution of nonpolar solvents and follows the order $PF_6^- < BF_4^- < CF_3SO_3^- < Cl^-$. Observed consequences are (*i*) a remarkable dependency of the spectroscopic characteristics (proton resonances and absorption bands) of the platinum cation on the nature of the counterion X^- and (ii) the possibility of measuring, for the first time, the rates of anion exchange at the NH site (Cl^- for PF_6^-), using conventional spectrophotometric techniques. Ion-pairing at the periphery of the ancillary ligand and even complete deprotonation have little effect on the reactivity. Thus, the ion-pairs **2**−**4** and the amido species **6** exchange dimethyl sulfoxide at comparable rates in chloroform. The labilizing effect of the amido group that dominates the dissociatively activated base-catalyzed reactions of octahedral complexes is absent.

Acknowledgment. We are grateful to the MURST and the CNR for funding this work.

Supporting Information Available: Figure S1 reporting a spectrophotometric titration of **2**, Figure S2 showing the dependence of the rates of ligand exchange on $[Me_2SO]$ for compounds **2**−**4** and **6**, Figure S3 reporting a correlation plot of the rates of substitution reactions of **2** and of the parent 1,10-phenanthroline complex, and Figure S4 showing the unit cell of compound **4**; tables giving complete crystallographic data, bond distances, bond angles, anisotropic thermal parameters, and hydrogen atom coordinates; Table S6 and Table S7 giving pseudo-first-order rate constants for dimethyl sulfoxide exchange on **2**−**4** and **6** and nucleophilic substitution on **2**, respectively; Table S8 reporting absorptions bands of compounds **2**−**5** and **6** (14 pages). Ordering information is given on any current masthead page.

IC980423Q

(26) (a) Tobe M. L. In *Comprehensive Coordination Chemistry*; Wilkinson, G., Ed.; Pergamon: Oxford, U.K., 1987; Vol. 1, pp 311−329; pp 47−75. (b) Tobe M. L. *Adv. Inorg. Bioinorg. Mech.* **1984**, *2*, 1. (c) Wilkins R. G. *Kinetics and Mechanisms of Reactions of Transition Metals Complexes;* VCH: Weinheim, Germany, 1991.